Hindawi
Shock and Vibration
Volume 2021, Article ID 9589230, 9 pages
https://doi.org/10.1155/2021/9589230

Research Article

Nonlinear Dynamics of the Rigid Drum for Vibratory Roller on Elastic Subgrades

Lun Liu,[1] Fenghui Wang,[2] Shupeng Sun ,[2,3] Weiming Feng,[2] and Chao Guo[3]

[1]*Institute of Dynamics and Control Science, Shandong Normal University, Jinan 250014, China*
[2]*School of Civil Engineering, Shandong University, Jinan 250061, China*
[3]*R&D Center, Shantui Construction Machinery Co. Ltd., Jining 272073, China*

Correspondence should be addressed to Shupeng Sun; shpsun@sdu.edu.cn

Received 9 September 2021; Accepted 10 November 2021; Published 30 November 2021

Academic Editor: Hulun Guo

In this paper, a coupling nonlinear dynamic model of the drum and subgrade is established for the vibratory roller. The dynamic characteristics of the rigid drum of the vibratory roller in the process of vibratory compaction are comprehensively investigated by time history, phase diagram, frequency spectrum, Poincare map, and bifurcation diagram. During the compaction process, the stiffness of the subgrade increases and the motion of the rigid drum of the vibratory roller changes from a single period to multiple periods and finally enters chaos by the way of period doubling. Moreover, the roller parameters also significantly affect the dynamic characteristics of the rigid drum and the compaction effect of the subgrade. Based on detailed numerical results, a parameter adjustment strategy about the roller frequency and nominal amplitude is proposed, which can avoid the "bouncing" of the drum during compaction and improve the compaction efficiency.

1. Introduction

Vibratory roller is one kind of common road construction machinery. The compaction operation of the vibratory roller is associated with the dynamic interaction between the vibratory roller and the subgrade. Consequently, to improve the compaction efficiency, it is of great importance to study the dynamics of the rigid drum for the vibratory roller on elastic subgrades.

The research on the dynamic characteristics of the rigid drum during compaction is always in progress. Yoo and Selig [1] firstly proposed a two-degree-of-freedom linear dynamic model by simplifying the drum of the vibratory roller and subgrade. However, the case of the drum leaving the subgrade is not taken into account in this linear model. Later, many researchers [2–5] proposed various vibration compaction models, including the nonlinear elastic model, the viscoelastic plasticity vibration compaction model, and the nonlinear hysteretic model. van Susante and Mooney [6] modeled the drum/soil system using the lumped parameter method and captured the complex nonlinear behavior of the system through simulation. Subsequently, Mooney and Rinehart [7, 8] collected data from field experiments to explore the relationship between vibration characteristics and subgrade stiffness. Furthermore, Kenneally et al. [9] investigated the interaction between the vibratory drum and the layered soil using finite element analysis, and the chaotic behavior and drum rocking were shown. Moreover, Yang et al. [10] studied the transmission and evolution characteristics of vibration waves in the process of vibration compaction based on the field experimental data of subgrade compaction engineering prototype. From these studies, one can see that although some of them address the dynamic characteristics of the vibratory roller, the parametric analysis of the dynamics of the drum/soil system is seldom involved.

To evaluate the compaction efficiency, various compaction indexes were proposed by researchers [11–13], and these compaction evaluation indexes were used to change the operating parameters of the vibratory roller in the process of compaction to maximize compaction efficiency. Anderegg and Kaufmann [14, 15] studied the nonlinear vibration of the vibratory roller and gave suggestions on the

control parameters of the vibratory roller. Zheng et al. [16] analyzed the influence of excitation amplitude and frequency and soil parameters on the dynamics of the vibratory drum. Based on the asymmetric hysteretic model of the compaction system, Shen et al. [4, 17] studied the chaotic vibration responses of the compaction system and showed the "bouncing" motion which can make the surface layer of subgrade loose and reduce the compaction efficiency. From these articles, it is observed that the adjustment strategy of operating parameters for vibratory rollers to avoid the bad operating condition, such as "bouncing," is scarcely reported in the open literature.

In this paper, a practical single-degree-of-freedom vibratory compaction model is used to analyze the dynamic characteristics of the rigid drum of the vibratory roller during the vibratory compaction process and to study the nonlinear dynamic behavior of the vibratory roller on elastic subgrades with different stiffness. Moreover, aiming at the "bouncing" phenomenon of rigid drum in the process of compaction, a parameter adjustment strategy of excitation frequency and nominal amplitude is proposed.

2. The Drum-Subgrade Coupling Dynamic Model

The drum-subgrade coupling model studied in this paper is shown in Figure 1. In this paper, we assume that the subgrade has been compacted many times, and the subgrade has changed from the original elastoplastic subgrade to elastic subgrade. For a vibratory roller, the support frame of the drum is an elastic frame, which is connected to the drum by a spring damping system. However, due to the damping effect of the spring damping system, the dynamic forces of the support frame have little effect on the drum response. According to relevant literature [8], the frame inertia is too small to be often neglected. Moreover, the dynamic forces from the drum-frame suspension are also small and can be neglected. Therefore, for the support frame, only the gravity of the frame mass is considered.

In this model, m_f and m_d denote the mass of the frame and the rigid drum of the roller, respectively. Inside the drum, there is an eccentric block with mass m_e and eccentricity r_e. The eccentric block rotates about the central axis of the drum at angular velocity Ω.

The vertical excitation force generated by the rotation of the eccentric mass block can be expressed as

$$F(t) = A_0 m_d \Omega^2 \cos(\Omega t), \tag{1}$$

where $A_0 = m_e r_e / m_d$ represents the nominal amplitude of the roller.

In the model, the displacement of the rigid drum in the vertical direction is denoted by x_d, which is measured from the uncompacted subgrade surface. According to Newton's second law, the equation of the vertical motion of the drum can be expressed as

$$m_d \ddot{x}_d + F_s - \left(m_d + m_f\right) g = A_0 m_d \Omega^2 \cos(\Omega t), \tag{2}$$

where F_s is the drum-subgrade interaction force. Its expression is given corresponding to the following cases.

Case I: when the drum of the vibratory roller is in contact with the subgrade, the contact force F_s can be expressed as

$$F_s = c_s \dot{x}_d + k_s x_d. \tag{3}$$

Case II: when the drum of the vibratory roller is out of contact with the subgrade, there is no contact force, i.e.,

$$F_s = 0. \tag{4}$$

3. Numerical Results and Discussion

This section firstly studies the dynamic characteristics of the drum during compaction in which the subgrade stiffness increases gradually. Next, through comparative analysis, the adjustment scheme of drum parameters is obtained, which makes the drum retreat from the state of "bouncing" once the drum bounces. The simulation parameters of the vibratory roller used are listed in Table 1. f is the excitation frequency of the vibratory roller. The unit used in this paper is the common representation of roller engineering application (1 MN/m = 1×10^6 N/m and 1 kNs/m = 1×10^3 Ns/m).

Figure 2 shows the bifurcation diagram of the drum response obtained by using the subgrade stiffness k_s as control parameter, and the subgrade damping is c_s = 130 kNs/m. It can be observed from the bifurcation diagram that the drum vibrates with a single period at the interval of k_s = 60 − 71 MN/m. Figure 3 shows the time history, phase diagram, frequency spectrum, and Poincare map for k_s = 60 MN/m. Figure 4 shows the corresponding contact force F_s. It can be seen from Figures 3(a) and 4 that when k_s = 60 MN/m, the value of drum displacement x_d is always positive and the contact force always exists. This means that the drum always vibrates below the surface of the uncompacted subgrade, i.e., the drum remains in contact with the subgrade during the compaction process. The frequency spectrum in Figure 3(c) only contains the dominant frequency component (32 Hz), and the drum moves in a single period without the phenomenon of "bouncing." When k_s = 70 MN/m, the numerical results are shown in Figures 5 and 6. It can be seen that the drum periodically lost contact with the subgrade surface, and the drum motion is still single periodic. At the interval of k_s = 71 − 76.5 MN/m, the drum is in the period two-movement window as shown in Figure 2. The detailed responses for k_s = 75 MN/m in this interval are illustrated in Figures 7 and 8. It can be observed that the drum displacement exceeds the uncompacted subgrade surface, and 1/2 of the vibratory frequency appears in the frequency spectrum. Moreover, two peaks occur in the curve of the contact force periodically. This means that the motion of the drum appears to be "bouncing." With the increase of k_s, the bifurcation diagram becomes more complicated, and the motion enters chaos finally, as shown in Figures 9 and 10 ($k_s = 85MN/m$). To sum up, the motion of the drum experiences the bifurcation from a single-period

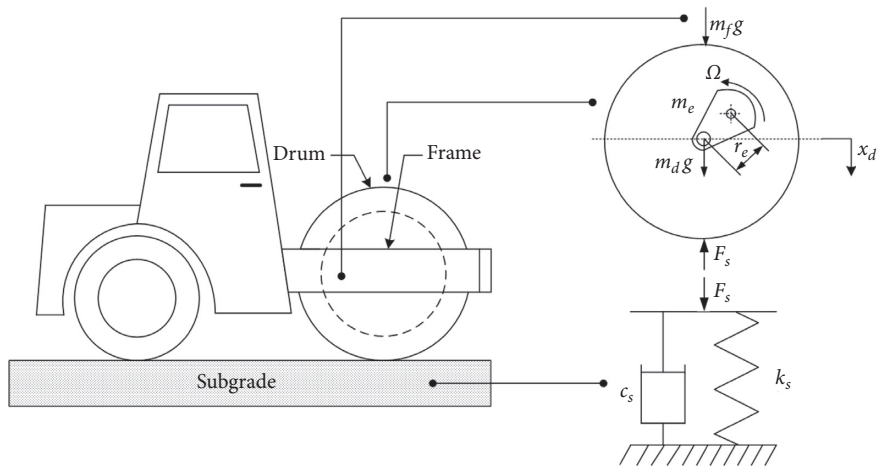

Figure 1: The drum-subgrade coupling dynamic model.

Table 1: Compaction model parameters.

Parameter	Symbol	Value
Drum mass	m_d	6450 kg
Frame mass	m_f	6354 kg
Excitation frequency	$f = \Omega/2\pi$	32 Hz
Nominal amplitude	A_0	1.5×10^{-3} m

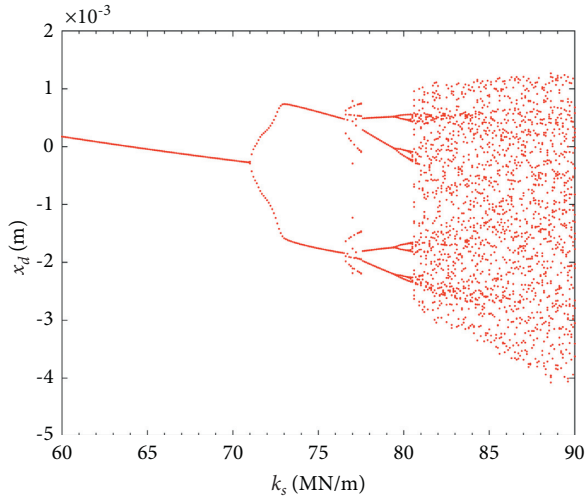

Figure 2: Bifurcation diagram with the subgrade stiffness k_s as the bifurcation parameter.

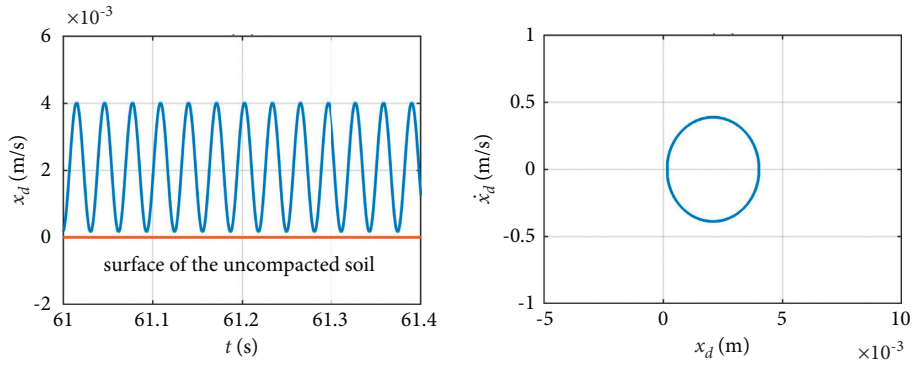

Figure 3: Continued.

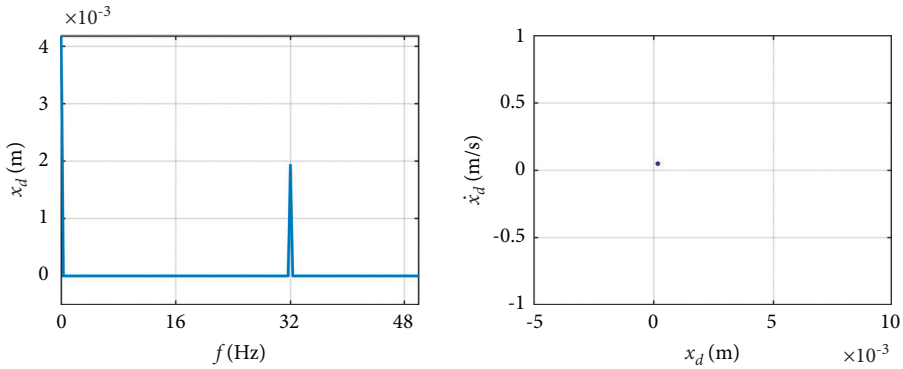

Figure 3: Dynamic responses of the rigid drum (k_s = 60)MN/m: (a) time history, (b) phase diagram, (c) frequency spectrum, and (d) Poincare map.

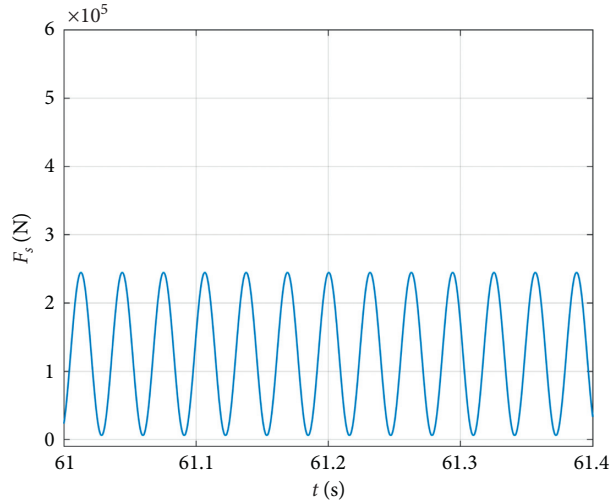

Figure 4: The contact forces F_s (k_s = 60 MN/m).

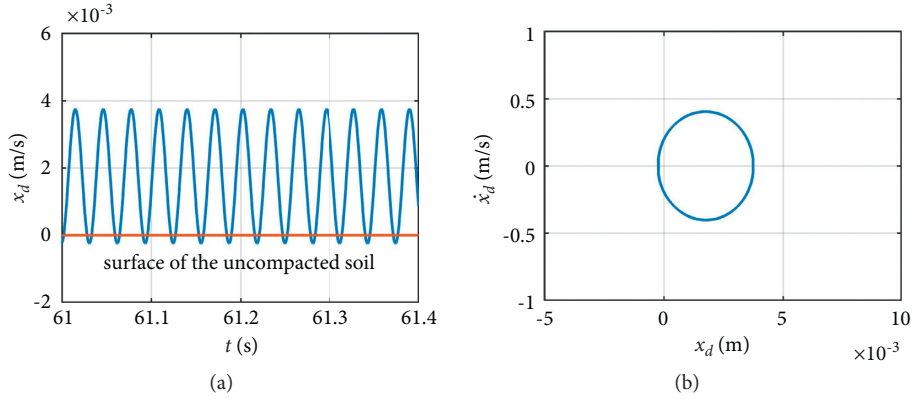

Figure 5: Continued.

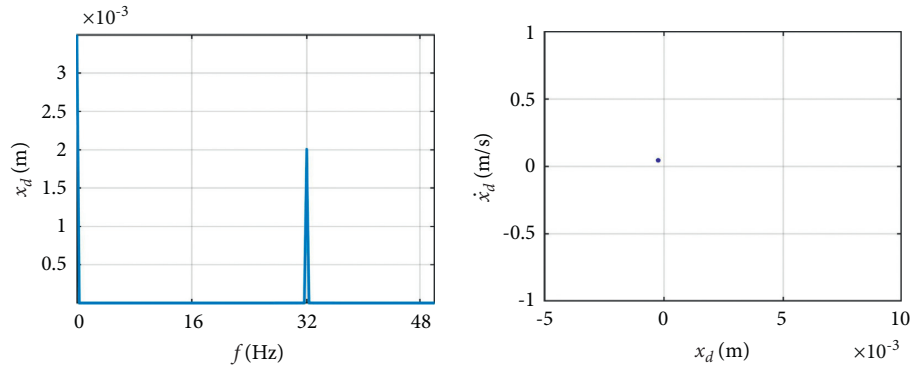

Figure 5: Dynamic responses of the rigid drum (k_s = 70)MN/m: (a) time history, (b) phase diagram, (c) frequency spectrum, and (d) Poincare map.

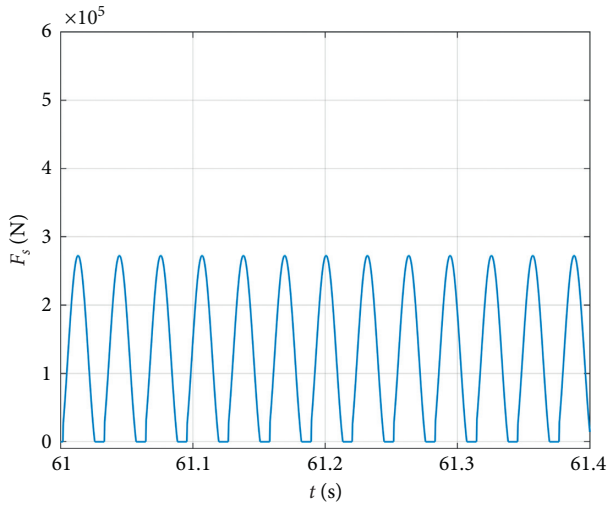

Figure 6: The contact forces F_s (k_s = 70 MN/m).

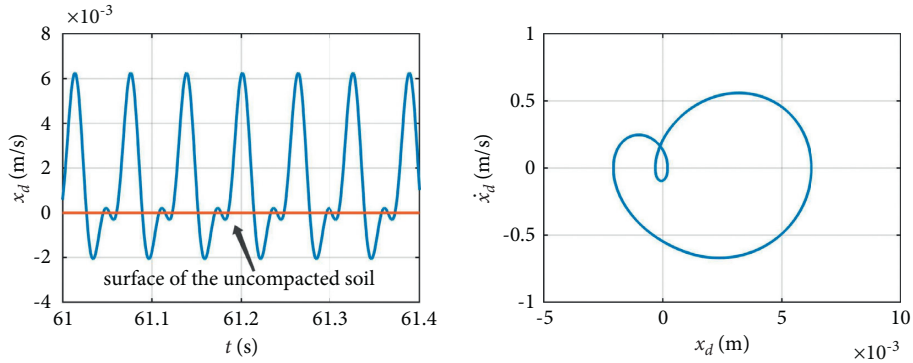

Figure 7: Continued.

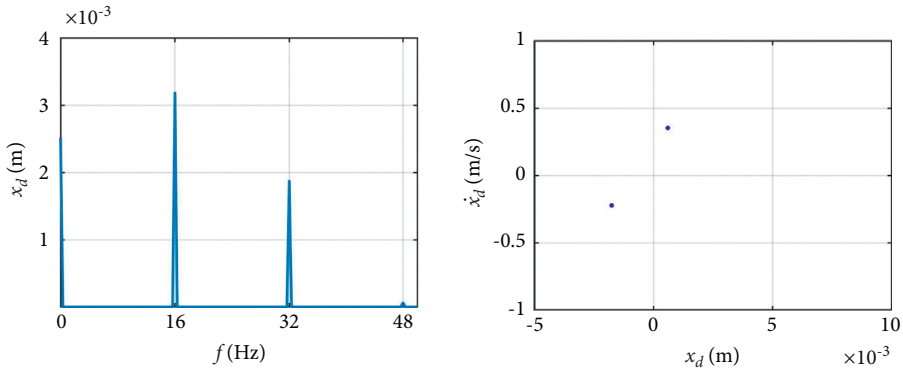

Figure 7: Dynamic responses of the rigid drum (k_s = 75)MN/m: (a) time history, (b) phase diagram, (c) frequency spectrum, and (d) Poincare map.

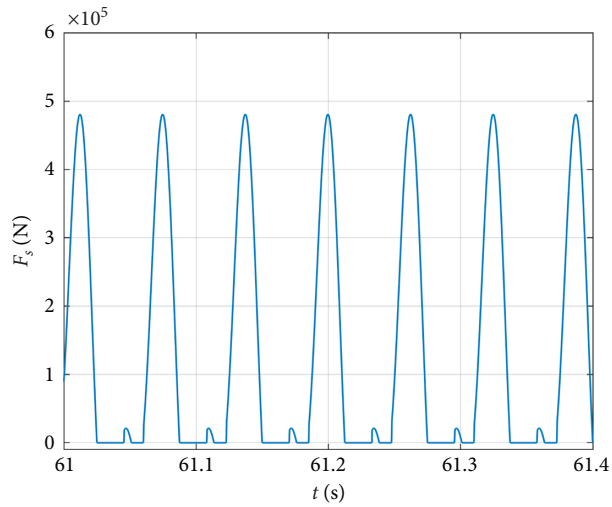

Figure 8: The contact forces F_s (k_s = 75 MN/m).

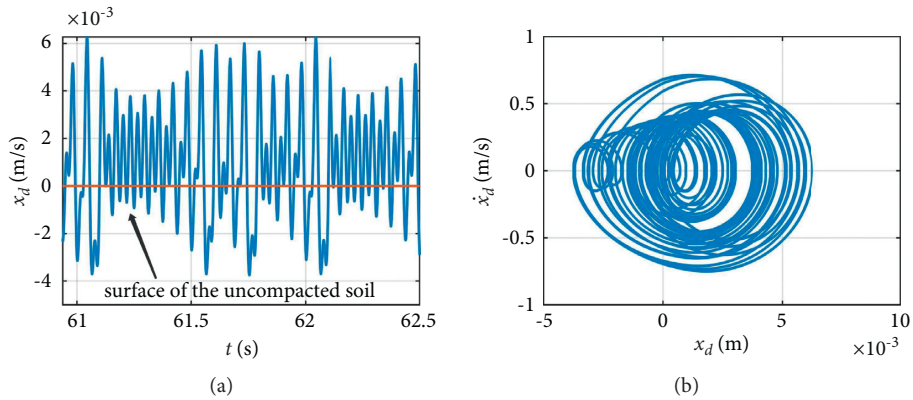

Figure 9: Continued.

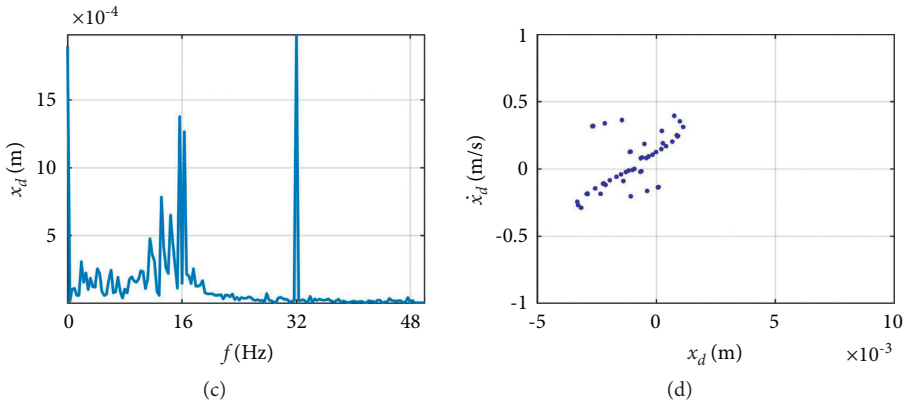

Figure 9: Dynamic responses of the rigid drum (k_s = 85)MN/m: (a) time history, (b) phase diagram, (c) frequency spectrum, and (d) Poincare map.

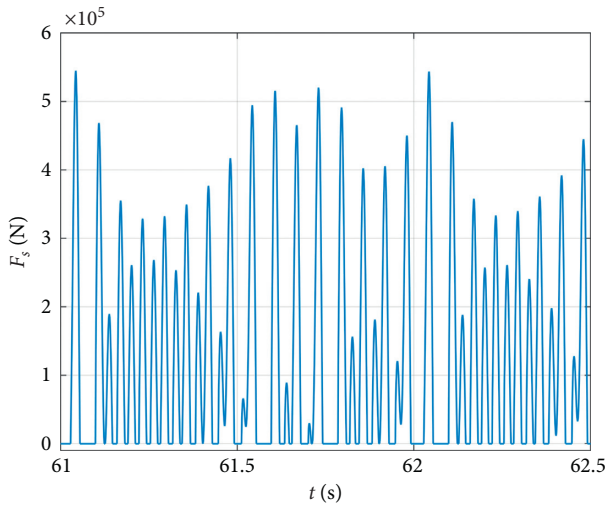

Figure 10: The contact forces F_s (k_s = 85 MN/m).

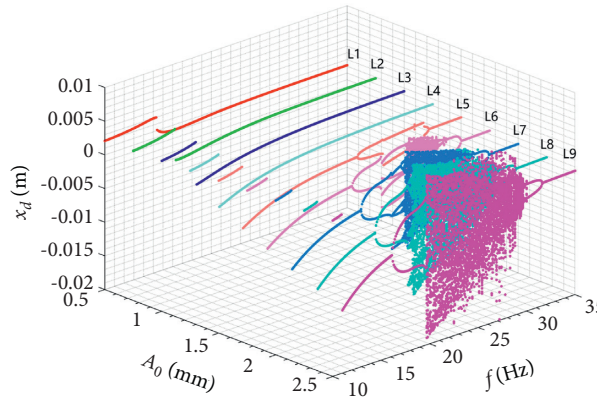

Figure 11: Bifurcation diagrams with excitation frequency f as bifurcation parameter under different nominal amplitudes (k_s = 70 MN/m and c_s = 130 kNs/m).

motion to multiperiod motion and finally enters chaos through the period-doubling bifurcation with the continuous increase of the subgrade stiffness. During this process, the drum experienced the change from contact, periodical loss of contact, and finally to the "bouncing" state which causes harmful compaction to the subgrade. Besides, bifurcation in the bifurcation diagram means that the drum exhibits "bouncing" phenomenon.

Figure 11 shows a three-dimensional image composed of nine bifurcation diagrams (L1–L9) of the drum responses, at point k_s = 70 MN/m and c_s = 130 kNs/m, by using excitation frequency f as the bifurcation parameter. When the nominal amplitude and excitation frequency are small, the drum always presents a single-period motion. In the cases of large nominal amplitudes, with the increase of excitation frequency, the dynamic response of the drum turns from a single period to multiple periods, even into chaos, and finally returns to the single-period motion. Moreover, with the increase of the nominal amplitude, the excitation frequency value of "bouncing" becomes smaller. Figures 12(a) and 12(b) show the bifurcation diagrams with nominal amplitude A_0 = 1 mm and 2 mm, respectively. From this figure, it can be found that the jumping phenomenon appears in the drum motion with the change of the excitation frequency. When the nominal amplitude increases, the excitation frequency gradually decreases when the jumping phenomenon occurs. For example, it can be seen from Figure 8 that the jumping phenomenon at the nominal amplitude of 2 mm occurs earlier than that at the nominal amplitude of 1 mm. From the above analyses, one can conclude that provided the stiffness of the subgrade is certain, once the drum exhibits "bouncing" motion, it can be removed from this state by reducing the nominal amplitude or by reducing/increasing the excitation frequency.

Figures 13 and 14 show two three-dimensional images composed of several bifurcation diagrams of the drum responses obtained by using the subgrade stiffness k_s as the bifurcation parameter. For Figure 13, A_0 = 1.5 mm, c_s = 130 kNs/m, and the interval of excitation frequency f is 10–35 Hz. From this figure, one can find that there is no bifurcation in the bifurcation diagrams for the low f and the drum keeps single periodic motion. However, with the increase of f, bifurcation would occur, and the value of

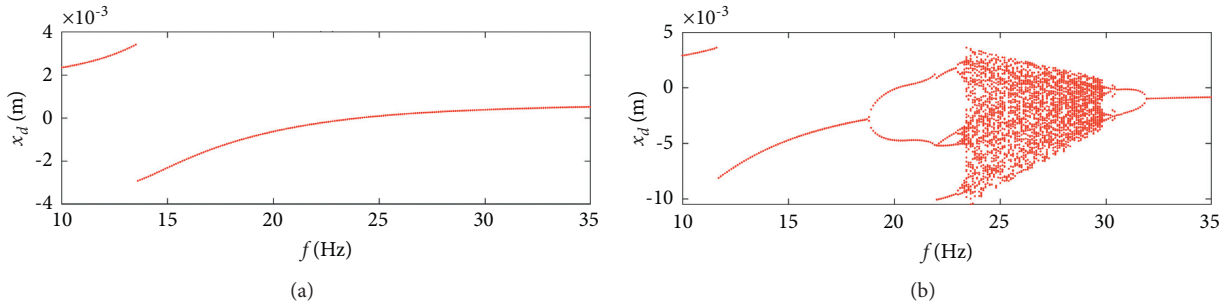

Figure 12: Bifurcation diagrams with excitation frequency f as bifurcation parameter (k_s = 70MN/m and c_s = 130kNs/m): (a)A_0 = 1 mm; (b)A_0 = 2 mm.

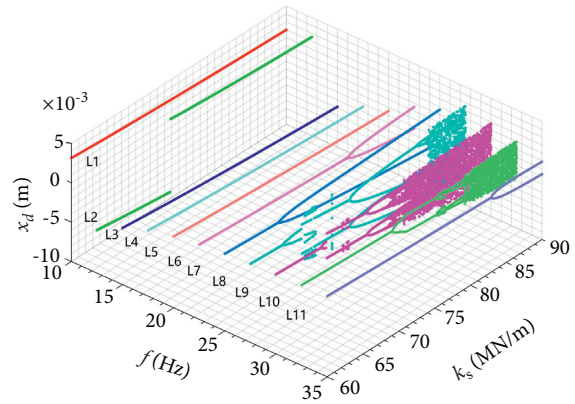

Figure 13: Bifurcation diagrams with the subgrade stiffness k_s as bifurcation parameter under different excitation frequencies (A_0 = 1.5 mm and c_s = 130kNs/m).

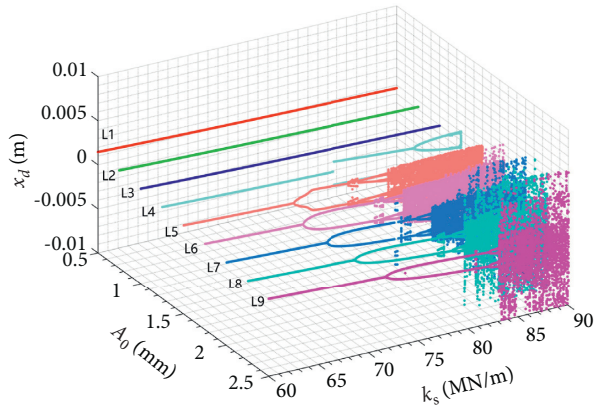

Figure 14: Bifurcation diagrams with the subgrade stiffness k_s as bifurcation parameter under different nominal amplitudes (f = 32 Hz and c_s = 130kNs/m).

subgrade stiffness k_s corresponding to the first bifurcation point for those bifurcation diagrams decreases first and then increases. This means that the "bouncing" motion of the drum is difficult to appear for a large subgrade stiffness when the excitation frequency is low/high. Because the compaction efficiency is low when the vibratory roller operates in the low-frequency range, the better choice would be increasing excitation frequency to avoid the drum "bouncing" motion for large subgrade stiffness. In Figure 14, f = 32 Hz, c_s = 130 kNs/m, and the interval of the nominal amplitude A_0 is 0.5–2.5 mm. It can be seen from this figure that the drum keeps a single periodic motion throughout the whole process of compaction, and no "bouncing" occurs to the drum when the nominal amplitude A_0 is small. With the increase of A_0, bifurcation would appear in the bifurcation diagrams, and the values of subgrade stiffness k_s corresponding to the first bifurcation point for those bifurcation cases are almost the same. From the above analyses, one can conclude that larger excitation frequency f and smaller nominal amplitude A_0 should be selected to avoid the drum "bouncing" motion and to improve the compaction efficiency in the later stage of compaction.

4. Conclusions

In this research, a coupling nonlinear dynamic model of the rigid drum and the subgrade is established for the vibratory roller, and the time history, phase diagram, frequency spectrum, Poincare section, and bifurcation diagram of drum responses are obtained to investigate dynamic characteristics of the rigid drum. Parametric studies are also carried out. According to those analyses, a parameter adjustment strategy is proposed to avoid the drum "bouncing" motion and improve the compaction efficiency. Some main conclusions are summarized as follows:

(1) The subgrade stiffness would increase gradually with the compaction progress. The motion of the rigid drum experiences the bifurcation from single-period motion to multiperiod motion and finally enters chaos. During this process, the drum experienced the change from contact, periodical loss of contact, and finally to the "bouncing" state.

(2) For a certain stiffness of the subgrade, one can draw the drum out of the "bouncing" motion state by reducing the nominal amplitude A_0 or by decreasing/increasing the excitation frequency.

(3) In the later stage of compaction progress, the larger excitation frequency and smaller nominal amplitude should be selected to avoid the drum "bouncing" motion and to improve the compaction efficiency.

Data Availability

The raw and processed data required to reproduce these findings are available from the corresponding author upon request.

Conflicts of Interest

The authors declare that they have no conflicts of interest.

Acknowledgments

This study was supported by the National Natural Science Foundation of China (grant nos. 11802129 and 11902184), the Shandong Provincial Natural Science Foundation of China (grant no. ZR2020QA039), and the Fundamental Research Funds of Shandong University. The authors are grateful for the financial support.

References

[1] T.-S. Yoo and E. T. Selig, "Dynamics of vibratory-roller compaction," *Journal of the Geotechnical Engineering Division*, vol. 105, no. 10, pp. 1211–1231, 1979.

[2] J. M. Machet and G. Morel, *Vibratory Compaction of Bituminous Mixes in France, Association of Asphalt Paving Technologists Proc*, pp. 326–340, Transportation Research Board, Washington, D.C., 1977.

[3] D. Pietzsch and W. Poppy, "Simulation of soil compaction with vibratory rollers," *Journal of Terramechanics*, vol. 29, no. 6, pp. 585–597, 1992.

[4] P.-H. Shen and S.-W. Lin, "Mathematic modeling and characteristic analysis for dynamic system with asymmetrical hysteresis in vibratory compaction," *Meccanica*, vol. 43, no. 5, pp. 505–515, 2008.

[5] F. Beainy, S. Commuri, M. Zaman, and I. Syed, "Viscoelastic-plastic model of asphalt-roller interaction," *International Journal of Geomechanics*, vol. 13, no. 5, pp. 581–594, 2013.

[6] P. J. van Susante and M. A. Mooney, "Capturing nonlinear vibratory roller compactor behavior through lumped parameter modeling," *Journal of Engineering Mechanics*, vol. 134, no. 8, pp. 684–693, 2008.

[7] M. A. Mooney and R. V. Rinehart, "Field monitoring of roller vibration during compaction of subgrade soil," *Journal of Geotechnical and Geoenvironmental Engineering*, vol. 133, no. 3, pp. 257–265, 2007.

[8] M. A. Mooney and R. V. Rinehart, "In situ soil response to vibratory loading and its relationship to roller-measured soil stiffness," *Journal of Geotechnical and Geoenvironmental Engineering*, vol. 135, no. 8, pp. 1022–1031, 2009.

[9] B. Kenneally, O. M. Musimbi, J. Wang, and M. A. Mooney, "Finite element analysis of vibratory roller response on layered soil systems," *Computers and Geotechnics*, vol. 67, pp. 73–82, 2015.

[10] C. Yang, L. Zhang, Y. Han, D. Cai, and S. Wei, "Study on the transmission and evolution characteristics of vibration wave from vibratory roller to filling materials based on the field test," *Applied Sciences*, vol. 10, no. 6, p. 2008, 2020.

[11] Q. Xu, G. K. Chang, and V. L. Gallivan, "Development of a systematic method for intelligent compaction data analysis and management," *Construction and Building Materials*, vol. 37, no. 37, pp. 470–480, 2012.

[12] W. Hu, B. Huang, X. Shu, and M. Woods, "Utilising intelligent compaction meter values to evaluate construction quality of asphalt pavement layers," *Road Materials and Pavement Design*, vol. 18, no. 4, pp. 980–991, 2017.

[13] T. B. Hua, X. G. Yang, Q. Yao, and H. T. Li, "Assessment of real-time compaction quality test indexes for rockfill material based on roller vibratory acceleration analysis," *Advances in Materials Science and Engineering*, vol. 2018, p. 15, Article ID 2879321, 2018.

[14] R. Anderegg and K. Kaufmann, "Intelligent compaction with vibratory rollers: feedback control systems in automatic compaction and compaction control," *Transportation Research Record: Journal of the Transportation Research Board*, vol. 1868, no. 1, pp. 124–134, 2004.

[15] R. Anderegg, D. A. Von Felten, and K. Kaufmann, "Compaction monitoring using intelligent soil compactors," *GeoCongress*, , pp. 41–46, Geotechnical Engineering in the Information Technology Age, 2006.

[16] S. Zheng, Q. Dai, and S. Lin, "Response characteristics analysis of vibrating drum in vibratory roller considering the asymmetrical hysteresis of materials," *Journal of Machine Design*, vol. 33, no. 9, pp. 87–91, 2016.

[17] P. Shen and S. Lin, "Mathematic modeling and chaotic identification for practice construction in vibratory compacting," *Journal of Vibration Engineering & Technologies*, vol. 6, no. 1, pp. 1–13, 2018.